

Supporting Information

Revealing the Structural Influence Mechanism of Intrinsic Potassium/Calcium Elements on Bio-waste-derived Hard Carbon for Sodium-ion Batteries

Yinghao Zhang^{a,b}, Chun Wu^{a,b,c}, Qinghang Chen^{a,b}, Chuangchuang Li^{a,b,c}, Wenjie Huang^{a,b}, Qianxiong Wen^{a,b}, Xiang-Xi He^b, Xingqiao Wu^{*a,b}, Shu-Lei Chou^{*a,b}

^a Institute for Carbon Neutralization Technology, College of Chemistry and Materials Engineering, Wenzhou University, Wenzhou, Zhejiang 325035, China

^b Wenzhou Key Laboratory of Sodium-Ion Batteries, Wenzhou University Technology Innovation Institute for Carbon Neutralization, Wenzhou, Zhejiang 325035, China

^c College of Materials Science and Engineering, Changsha University of Science and Technology, Changsha 410114, China

* Xingqiao Wu; Shu-Lei Chou

Email: xingqiaowu@wzu.edu.cn; Email: chou@wzu.edu.cn

Synthesis of hard carbon

The gourd shell is selected as the raw material for synthesizing hard carbon and the seeds are extracted from the gourd. Subsequently, the gourd shell is crushed into powder using a pulverizer, dried, and then stored under vacuum, named as MG. The MG is directly pyrolysis in a tubular furnace, heated in a N₂ at a ramping rate of 10 °C/min to 1000 °C, then ramped at 5 °C/min to 1200 °C, 1400 °C, 1600 °C, and maintained for 3 hours. The resulting hard carbon samples are named: MGHC-L, MGHC-M, MGHC-H (MGHC-X, where X represents different temperatures). Next, the same biomass material undergoes acid treatment. A 0.3 M H₂SO₄ solution is prepared in a beaker, and the raw material is added at a ratio of 10 g (gourd shell powder) to 200 mL (H₂SO₄ solution). The mixture is stirred magnetically at room temperature for 6 hours. Subsequently, it is washed with deionized water to remove excess H₂SO₄ until the pH reaches neutrality. The washed material is then dried in a blast oven for 12 hours, named as MG-A. MG-A is placed in the tubular furnace, and pyrolysis is carried out following the same steps as the MG, resulting in hard carbon materials named: MGHC-L-A, MGHC-M-A, MGHC-H-A (MGHC-X-A, where X represents different temperatures).

Electrode preparation and electrochemical measurements

The obtained hard carbon material is ground into powder with a mortar, and the active substance: sodium alginate (2 %) = 95: 5 ratio of the homogenate is shook and evenly coated on the aluminum foil with a scraper. The aluminum foil with slurry was then put into a vacuum oven and dried at 90 °C for 12h. After the slurry is dry, it is cut into 10mm pieces and stored in a glove box filled with Ar atmosphere after weighing. The content of active substance in the obtained electrode is about 1.7-1.9 mg cm⁻².

The assembly of the half battery Na||HC (CR-2032) is carried out in a glove box filled with Ar atmosphere, where the water and oxygen content are less than 0.01ppm. Glass cellulose fiber (GF/A, Whatman, UK) was used for the separators, and sodium metal was cut into 12 mm discs as the counter electrode used a knife. The electrolyte is

a solution obtained by dissolves 1 M NaPF₆ into a solvent of ethylene carbonate (EC) and dimethyl carbonate (DMC) (1:1 volume ratio).

The assemble process of the Na||Na₂MnFe(CN)₆ half-cell (CR-2032) is carried out in a glove box filled with Ar atmosphere, where the water and oxygen content are less than 0.01 ppm. Glass cellulose fiber (GF/A, Whatman, UK) is used for the separators, and sodium metal is cut into 12 mm discs as the counter electrode. The electrolyte is NTE-0005. (NTE-0005 electrolyte is purchased from Wenzhou NaTech New Energy Technology Co., Ltd)

The fabrication procedure of the full-cell (CR-2032) is carried out in a glove box filled with Ar atmosphere, where the water and oxygen content are less than 0.01ppm. The positive electrode is Na₂MnFe(CN)₆, and its coating ratio is: active material: carbon black: water-based adhesive (5%)=8: 1: 1, and it is cut into 10mm pieces after drying in vacuum oven. The negative electrode is MGHC-M-A, its coating ratio is: active material: SA (2%)=95: 5, and it is also cut into 10 mm pieces after drying in vacuum. The separator is glass cellulose fiber (GF/A, Whatman, UK), using the same electrolyte as the above half-cell. The N/P ratio of the full-cell is 1.02 under voltage range 1.6 - 3.6 V.

The electrochemical behavior measurements of half-cell Na||HC and full-cell Na₂MnFe(CN)₆||HC were carried out at room temperature constant current charge and discharge test by NEWARE battery test system (CT-4008T, Shenzhen, China). The constant current intermittent titration technology (GITT) uses the NEWARE battery test system (CT-4008T, Shenzhen, China) to discharge at the current density of 20mA g⁻¹ for 30 minutes in the voltage range of 0-2 V, and the standing time is 4 h.

Structural stability evaluation of hard carbon anode

The assembled half-cell Na||HC is charged and discharged at constant current on the NEWARE battery test system. The anode is obtained by disassembling the recycled battery. For ease of distinction, the anode after cycled is named as MGHC-M-A-After Cycling, while the original anode is named MGHC-M-A-Original.

Test ash-forming elements in Muffle furnace

In this paper, the ash-forming elements of MG, MG-A, MGHC-X and MGHC-X-A are all obtained by sintering in Muffle furnace (KSL-1200X-J, crystal). The sintering process is as follows: 1 g material was added to the corundum crucible, and the material was kept in the Muffle furnace at a heating rate of 5 °C min⁻¹ to 800 °C for 10 h, and the ash-forming elements were taken out after natural cooling.

Calculation of apparent Na⁺ chemical diffusion coefficients through GITT results

GITT is a technique for measuring ion diffusion and electron conduction in electrochemical systems. This method first applies a constant current, charges or discharges for a certain amount of time, then stops the current and measures the open circuit voltage or current response. The ion diffusion coefficient in the electrochemical process and the electrochemical properties of materials can be understood by analysis. The ionic diffusion coefficient is calculated as follows:

$$D = \frac{4}{\pi\tau} \left(\frac{m_B V_M}{M_B S} \right)^2 \left(\frac{\Delta E_S}{\Delta E_\tau} \right)^2 \quad (1)$$

In this formula: τ is the current pulse time, m_B is the electrode active material, V_M is the molar volume of the material, M_B is the molar mass of the material, S is the geometric area of the electrode sheet, ΔE_S is the voltage change caused by the pulse, ΔE_τ is the voltage change of constant current charge (discharge).

Materials characterization

X-ray powder diffraction (XRD) analysis was carried out using the Panalytical Aeris X-ray powder diffractometer with the Cu K α radiation, set at the operating voltage of 40 kV ($\lambda = 0.154$ nm) (Malvern Panalytical, Netherlands.), which was used to investigate the degree of graphitization of hard carbon materials and the size of the layer spacing. Raman spectra were analyzed using the Horiba XploRA™ PLUS spectrometer (France) with a laser at 532 nm wavelength. The micromorphology and elemental content of the materials were observed and measured by SEM3100 scanning

electron microscopy (SEM, China) and Energy Dispersive X-ray Spectroscopy (EDS, Xlpore, UK). The element content in the sample was accurately determined by ICP (Inductively Coupled Plasma) (Agilent 5100). N₂ adsorption and desorption were performed with Micrometrics ASAP 2460 volumetric gas adsorbent at 77 K to obtain the specific surface area and pore size of the material. The microstructure of the material was observed by FEI Tecnai G2 F20 transmission electron microscope. XPS (X-ray photoelectron spectroscopy) uses Thermo Scientific K-Alpha spectrometer and Al K-alpha X-ray source to detect surface chemical states. Small Angle X-ray scattering (SAXS) used Xeuss 2.0 (French Xenocs) to analyze the closed-cell structure of the material. The true density test uses the AccuPyc II 1340(USA), a fully automated true density tester, to measure the true density of a material without voidage or bubbles. ICP test used

Author contributions

Y. Z. and X. W. contributed to the experimental design. Y. Z. performed the electrochemical measurements and experiments for characterizing the hard carbon with the advice of Q. C. and C. L., Y. Z. complete the electrochemical tests W. H., Q. W. and X. X. H., Y. Z. wrote the first draft of the manuscript, X. W. supervised the study. All authors reviewed and revised the manuscript in several steps and approved the final version of the manuscript.

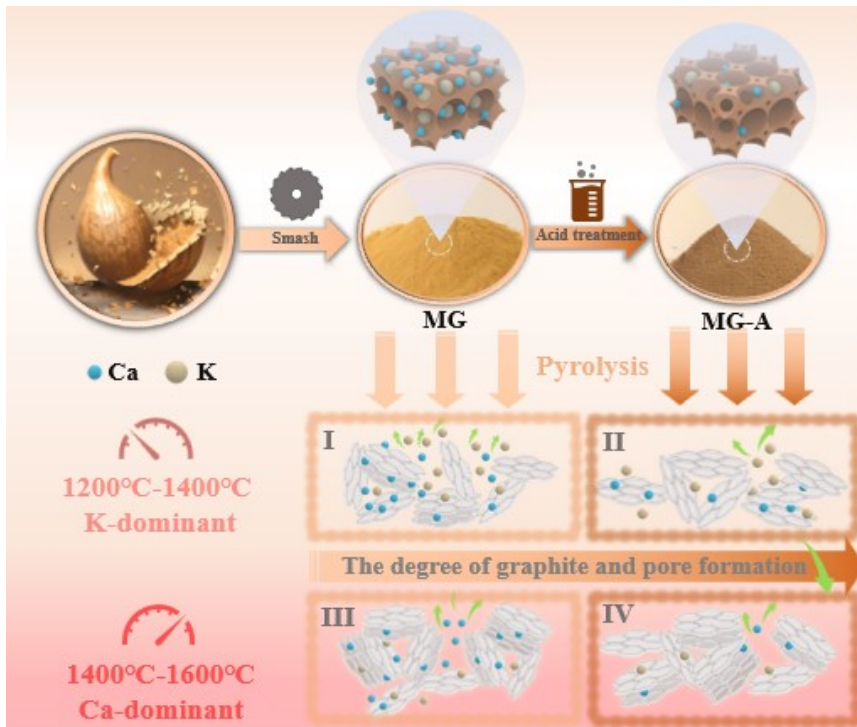


Fig. S1 Pretreatment of waste gourd shell and influence mechanism of ash-forming elements on microstructure in different pyrolysis zones before and after pretreatment.



Fig. S2 The photograph of a waste gourd

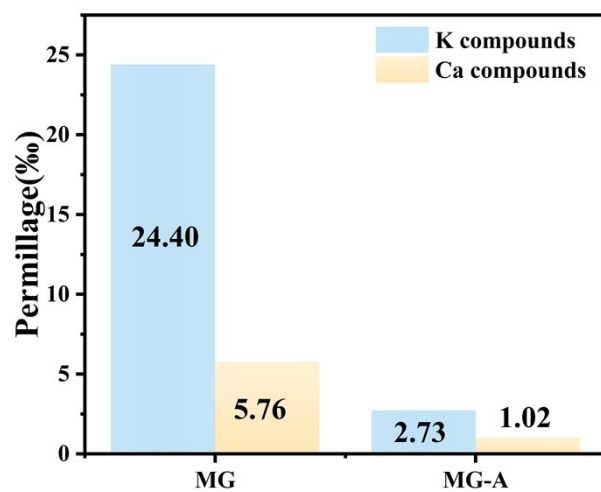


Fig. S3 Ash-forming elements content in (a) MG and (b) MG-A

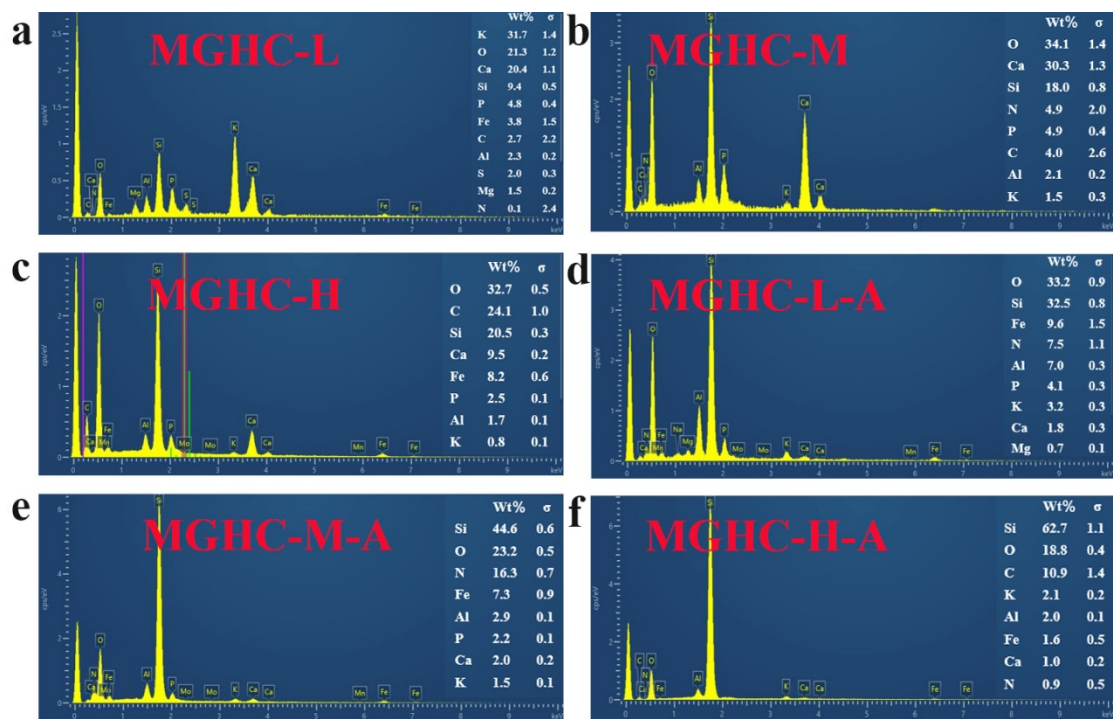


Fig. S4 EDS of ash-forming elements in MGHC-X and MGHC-X-A samples

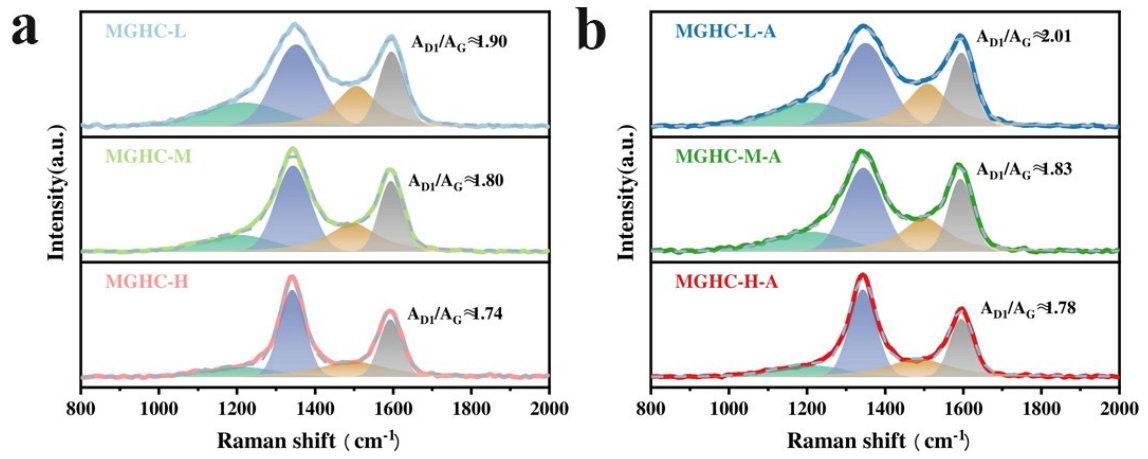


Fig. S5 Raman spectral peak analysis of (a) MGHC-X and (b) MGHC-X-A

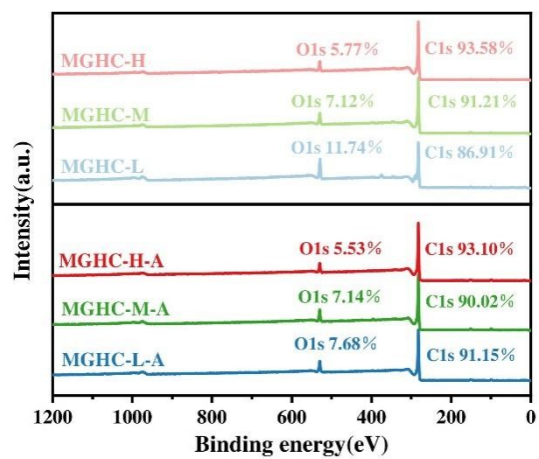


Fig. S6 XPS of MGHC-X and MGHC-X-A

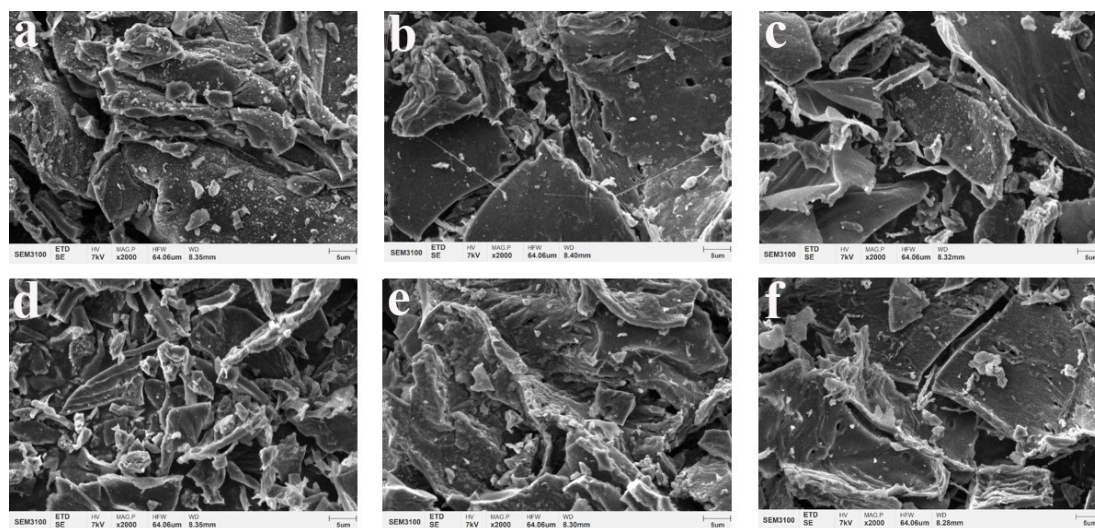


Fig. S7 The SEM images of (a) MGHC-L, (b) MGHC-M, (c) MGHC-H, (d) MGHC-L-A, (e) MGHC-M-A, (f) MGHC-H-A

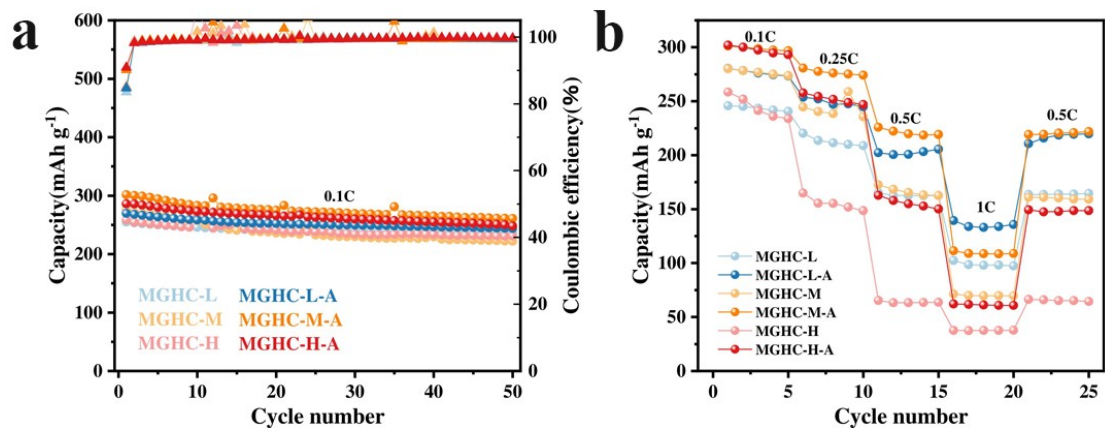


Fig. S8 (a) Cycling and (b) rate performance of MGHC-X and MGHC-X-A

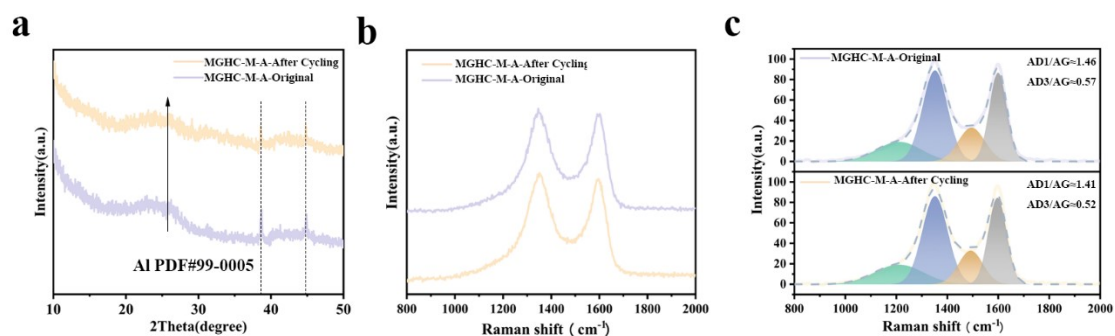


Fig. S9 (a) XRD, (b) Raman and (c) the fitting of Raman of MGHC-M-A-After Cycling and MGHC-M-A-Original

The XRD test shows that the 002 peaks before and after cycles are similar, indicating that the degree of graphitization exhibits no significant change. It is worth mentioning that the peak near 39° and 46° can be ascribed to the characteristic peak of Al, which is derived from the current collector. The AD1/AG obtained after Raman peak splitting also proves that the degree of graphitization after the cycles do not change significantly. Meanwhile, there is no significant change in AD3/AG, verifying the stability of the hard carbon anode.

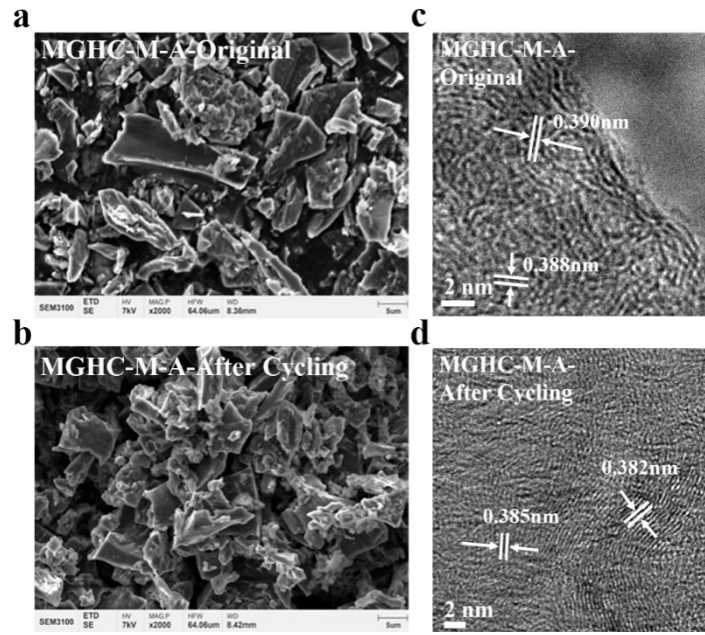


Fig. S10 (a, b) SEM images, (c, d) TEM images of MGHC-M-A-After Cycling and MGHC-M-A-Original

From the SEM and TEM images, there is no significant difference in morphology before and after cycles, suggesting that the microstructure of the hard carbon anode remains stable before and after cycles.

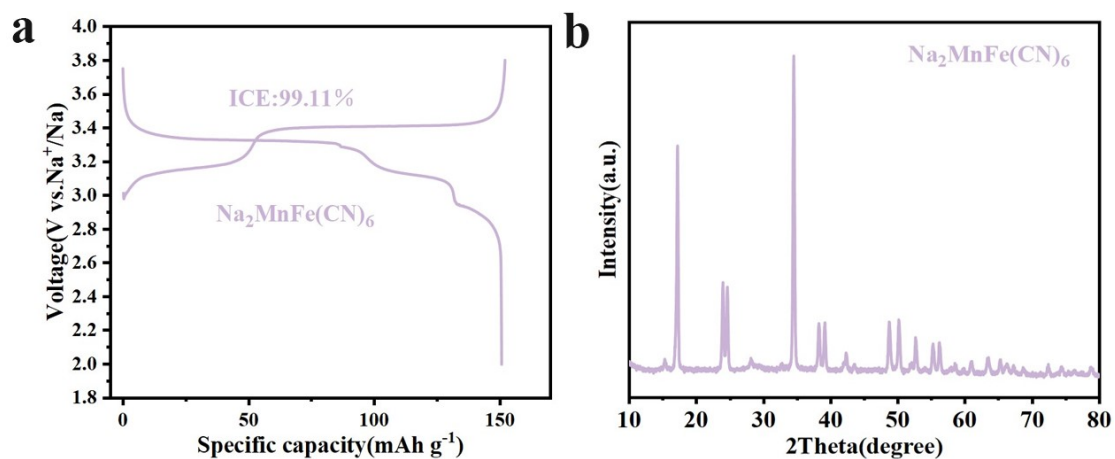


Fig. S11 (a) The charge/discharge curve of $\text{Na}_2\text{MnFe}(\text{CN})_6$ half-cell and (b) the XRD of $\text{Na}_2\text{MnFe}(\text{CN})_6$ cathode material

The split peaks are mainly distributed at 24.2° , 38.5° , 49.5° , 55.8° and these peaks are due to the -CN distortion in sodium-rich PBAs.

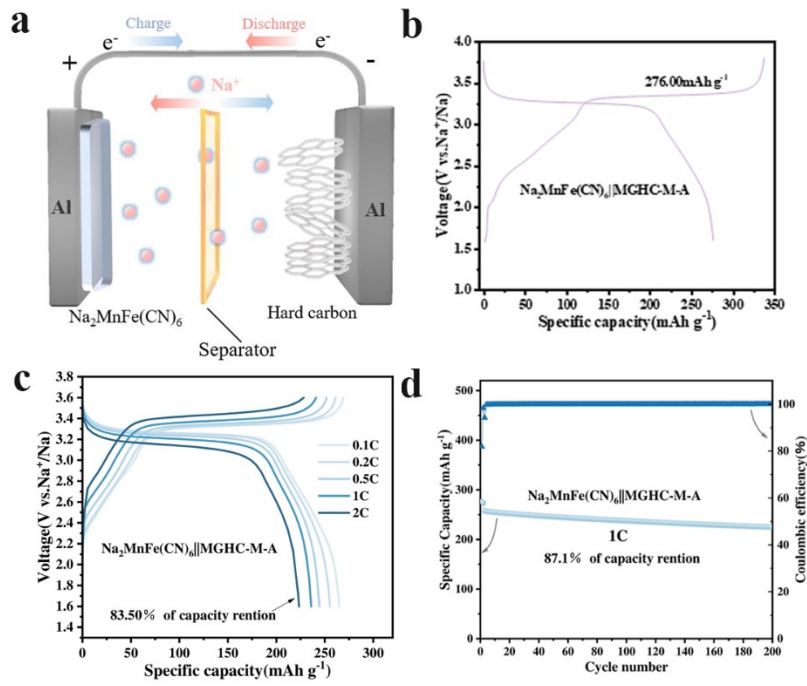


Fig. S12 (a) The working principle illustration of full cell, (b) the first cycle electrochemical curve of the full cell based on $\text{Na}_2\text{MnFe}(\text{CN})_6$ as the cathode and MGHC-M-A as the anode, (c) rate, (d) cycling behavior of $\text{Na}_2\text{MnFe}(\text{CN})_6$ ||MGHC-M-A full cell.

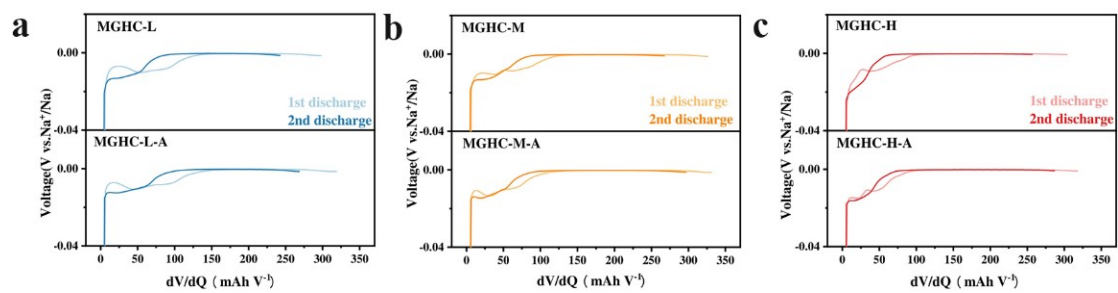


Fig. S13 (a-c) The first circle discharge and the second circle discharge of the dV/dQ curves for MGHC-X and MGHC-X-A.

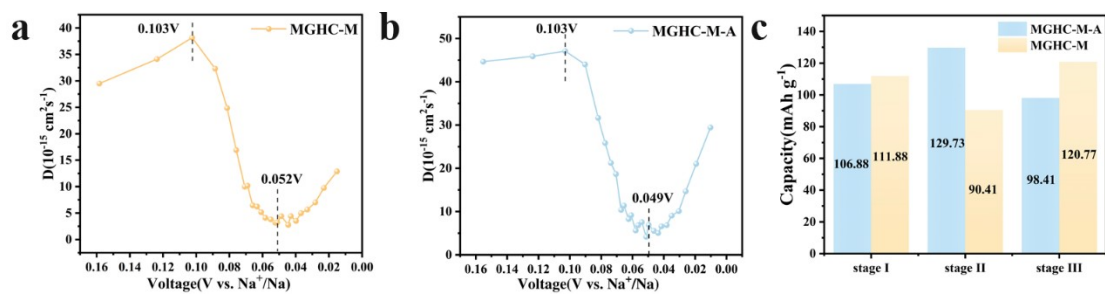


Fig. S14 (a, b) the diffusion coefficient and (c) the capacity distribution from first cycle discharge process of MGHC-M and MGHC-M-A

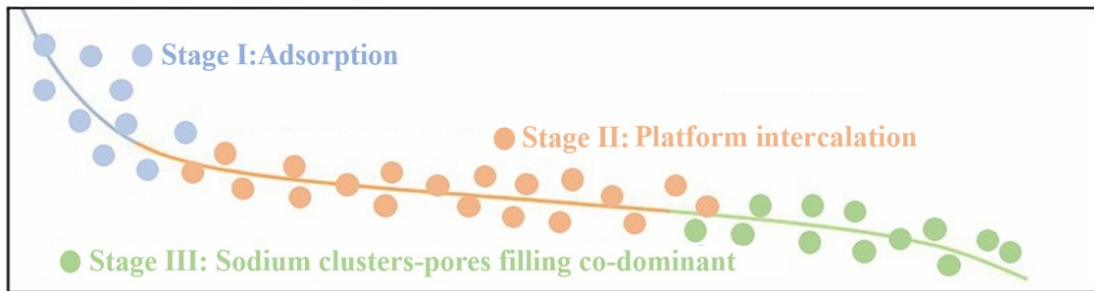


Fig. S15 Schematic diagram of sodium storage mechanism.

Table S1 The content of K and Ca compounds in MGHC-X and MGHC-X-A

Samples	K compounds (‰)	Ca compounds (‰)
MG	24.41	5.77
MG-A	2.73	1.02
MGHC-L	25.96	7.88
MGHC-M	3.68	6.93
MGHC-H	0.61	2.39
MGHC-L-A	1.00	0.66
MGHC-M-A	0.75	0.61
MGHC-H-A	0.12	0.23

Table S2. The SSA and pore volume of MGHC-X and MGHC-X-A

Samples	SSA (m ² g ⁻¹)	Pore volume (cm ³ g ⁻¹)
MGHC-L	5.96	0.015
MGHC-M	9.96	0.018
MGHC-H	36.71	0.043
MGHC-L-A	7.98	0.017
MGHC-M-A	4.59	0.008
MGHC-H-A	2.69	0.007

Table S3. The content of ash-forming elements in MGHC-X and MGHC-X-A

Samples	Ash-forming elements content (%)
MGHC-L	7.9
MGHC-M	7.6
MGHC-H	6.9
MGHC-L-A	3.3
MGHC-M-A	2.9
MGHC-H-A	2.8

Table S4. The boiling point of K and Ca compounds

Compound	KCl	K ₂ CO ₃	CaCl ₂	CaSO ₄
Boiling point (°C)	≈1420	≈ 1400	≈1600	≈1600

Table S5. The true density and closed pore volume of MGHC-M, MGHC-M-A, MGHC-H, MGHC-H-A

Sample	MGHC-M-A	MGHC-M	MGHC-H-A	MGHC-H
True density (g cm ⁻³)	2.25	2.13	1.93	1.85
Closed pore volume (cm ³ g ⁻¹)	0.002	0.027	0.076	0.098

Table S6. A_{D1}/A_G , A_{D3}/A_G parameters obtained after peak separation of the Raman spectra

Samples	A_{D1}/A_G	A_{D3}/A_G
MGHC-L	1.90	1.21
MGHC-M	1.80	1.16
MGHC-H	1.74	1.09
MGHC-L-A	2.01	1.28
MGHC-M-A	1.83	1.22
MGHC-H-A	1.78	1.14

Table S7. Rate capacity retention rate of MGHC-X and MGHC-X-A

Samples	0.2C (%)	0.5C (%)	1C (%)
MGHC-L	89.63	67.25	41.65
MGHC-L-A	90.52	72.21	49.77
MGHC-M	87.34	61.61	25.49
MGHC-M-A	93.20	75.01	37.01
MGHC-H	63.82	25.31	14.53
MGHC-H-A	85.37	53.95	20.60